Kent Academic Repository

Carta, Daniela, Pickup, David M., Knowles, Jonathan C., Smith, Mark E. and Newport, Robert J. (2005) *Sol-gel synthesis of the P2O5-CaO-Na2O-SiO2 system as a novel bioresorbable glass.* Journal of Materials Chemistry, 15 (21). pp. 2134-2140. ISSN 0959-9428.

Versions of research works

Sol–gel synthesis of the P_2O_5–CaO–Na_2O–SiO_2 system as a novel bioresorbable glass

Daniela Carta,*[a] David M. Pickup,[a] Jonathan C. Knowles,[b] Mark E. Smith[c] and Robert J. Newport[a]

A series of phosphate-based sol–gel glasses in the system P_2O_5–CaO–Na_2O–SiO_2 were synthesised using $PO(OH)_{3-x}(OC_2H_5)_x$ (x = 1, 2) as a phosphorus precursor and alkoxides of sodium, calcium and silicon in an ethylene glycol solution. It has been found that the upper limit for gel formation is about 22 mol% phosphorus and that the gelation time increases with increasing phosphorus content of the sol. X-ray diffraction (XRD) along with X-ray fluorescence chemical analysis (XRF) have been performed on samples containing 45 mol% of P_2O_5 and 0, 10, 15 and 25 mol% of SiO_2 with varying amount of modifier oxides (CaO, Na_2O). All the samples are predominantly amorphous up to 400 °C and some of them, depending on the composition, retain their amorphous structure up to 600 and 800 °C. To the knowledge of the authors, this is the first time that phosphate-based glasses having these compositions have successfully been synthesised *via* the sol–gel method.

1. Introduction

With increasing human life expectancy, an improvement in the quality of biomaterials used for regeneration or repair of hard and soft tissues in the human body is necessary. For instance, the number of people affected by bone diseases such as osteoporosis is dramatically increasing especially among the aged. As a result, the major clinical application of biomaterials is in the field of the treatment of bone defects (coating on metallic implants, bone grafting materials). The first generation of biomaterials, from the early 1970s, can be classified as bioinert. Designed to minimize any aggressive biological responses by the body, they simply had a mechanical role. During the 1980s, a second generation of biomaterials, defined as bioactive, was developed. Their key feature is the capability of their surface to interact with physiological fluids to generate a bone-like layer of hydroxyapatite $Ca_{10}(PO_4)_6(OH)_2$. Human cells grow and proliferate on this layer promoting a tight bond between the implant and the living tissue. Recently, a third generation of biomaterials has been developed. They can be defined as bioresorbable, as they react and dissolve in the physiological environment and they are eventually replaced by regenerated hard or soft tissue. A broad range of materials including ceramics, glass ceramics, polymers and glasses can act as biomaterials. The work reported herein is particularly focused on the synthesis and characterisation of new bioactive and bioresorbable glasses made using the sol–gel method.

The traditional bioactive glasses used in biomedical research have a silicate network with the main structure formed by $(SiO_4)^{4-}$ tetrahedra units linked by bridging oxygens. Because of their insolubility, they are used as long-term implants to replace hard or soft tissues. The first bioactive glasses presented by Hench *et al.*[1] in 1971 were synthesised by the melt-quenched route and had a composition based on SiO_2–P_2O_5–CaO–Na_2O, with silica as the main component, and many of the contemporary analogues, including those generated by sol–gel methods[2,3] have a SiO_2–CaO based structure. A new generation of bioresorbable glasses reported here are based on an inorganic phosphate network of $(PO_4)^{3-}$ tetrahedral sharing bridging oxygen rather than the traditional silica network. Because of their solubility, they can find application as degradable temporary implants that can be replaced by natural tissues. Systems with P_2O_5 as their main component, with the addition of modifier oxides such as CaO, Na_2O and K_2O have been recently synthesised[4–6] using a conventional melt-quenching route.

In the past decade, the sol–gel process has attracted increasing attention as an alternative synthetic route to the traditional melt-quenching method. Sol–gel synthesis offers low-temperature processing along with the homogenous mixing of the reactants, leading to better quality glasses with a more easily controlled morphology. However, whilst the sol–gel synthesis of silicates glasses has been extensively studied, much fundamental work remains to be done on the sol–gel synthesis of phosphates. The structure of phosphates in the crystalline phase is also based on tetrahedral units, but their chemical behaviour in solution is very different. The monophosphate unit $(PO_4)^{3-}$ appears to be a good glass-former but is not as good a gel-former as $(SiO_4)^{4-}$. Therefore, the sol–gel chemistry of phosphates is much more challenging than that of the silicates. The few papers hitherto published relating to the sol–gel synthesis of phosphosilicates mainly concern systems with silica as the predominant component. A range of phosphorus precursors has been used for the synthesis of these silica-based sol–gel materials. Woignier *et al.*[7] synthesised phosphosilicate aerogels with an amount of P_2O_5 between 5 and 50 mol% using methylphosphate as a precursor. Vallet-Regí *et al.*[8] prepared sol–gel glasses in the system 80 mol% SiO_2, 4 mol% P_2O_5 and either CaO and MgO as

*dc24@kent.ac.uk

the remainder, using triethylphosphate as precursor. Clayden et al.[9] used phosphoryl chloride $POCl_3$ as a precursor to synthesise systems with a molar composition of 90% SiO_2–10% P_2O_5 and 70% SiO_2–30% P_2O_5. The sol–gel synthesis of pure phosphates glasses or phosphosilicates having P_2O_5 as a main component is not as straightforward. The main problem is related to the difficulty of finding a suitable phosphorus precursor. As described in detail by Livage et al.[10] phosphoric acid, H_3PO_4, is too reactive towards water and usually leads to precipitation instead of gelation. On the other hand, the high stability of phosphate esters, $PO(OR)_3$, towards water make their hydrolysis reaction very slow. Szu et al.[11] studied the effect of the precursor on the synthesis of phosphosilicate gels with compositions between 5 and 90 mol% of P_2O_5. Using phosphoric acid, H_3PO_4, the upper limit for gel formation is 90 mol% of P_2O_5 but the gels having more than 15 mol% of P_2O_5 partially crystallise after heating at 200 °C. The same upper limit for gel formation is obtained using trimethylphosphite, $P(OCH_3)_3$, but all the gels, regardless of composition, fully crystallise at 200 °C. By using triethylphosphate, $PO(OC_2H_5)_3$, the upper limit for gel formation decreases to 70 mol% of P_2O_5 and the gels lose more than 90% of the initial amount of P_2O_5 during heating treatment. It has been suggested that alkyl phosphates such as $OP(OR)_x(OH)_{3-x}$ (x = 1, 2) or $P(OR)_3$ and phosphoryl chloride $POCl_3$ are more convenient precursors for the sol–gel synthesis of phosphates.[10] Nevertheless, phosphosilicate gels synthesised using $POCl_3$ as a precursor and containing just 30 mol% P_2O_5 crystallise after being heated at 400 °C for 30 min.[9] It has also been reported that the relative loss of phosphorus from the gel upon heating is higher using $P(OR)_3$ or $POCl_3$ than using $OP(OR)_x(OH)_{3-x}$ as a precursor.[12]

In the present work, phosphate glasses in the system P_2O_5 (40–50 mol%)–CaO (20–45 mol%)–Na_2O (5–35 mol%) and SiO_2 (0–25 mol%) have been synthesised by the sol–gel route using alkyl phosphate $OP(OR)_x(OH)_{3-x}$ (x = 1, 2) as the molecular precursor. To our knowledge, this is the first time that systems with compositions in this region have been synthesised via the sol–gel method. In particular, there is no evidence of the successful synthesis of amorphous phosphate sol–gels materials containing less than 25 mol% of silica published hitherto.

2. Experimental

2.1 Materials

The following chemicals have been used for the synthesis of sol–gel phosphates: phosphorus pentoxide (P_2O_5, Aldrich, 99.99+%), calcium methoxide ($Ca(CH_3O)_2$, Aldrich, 97%), sodium methoxide ($Na(CH_3O)$, Aldrich, 95%) and tetraethoxysilane ($Si(CH_3CH_2)_4$, Fluka, 99%). All the solvents used in this work had the lowest available water content: anhydrous ethanol (CH_3CH_2OH, Aldrich) had an amount of water (<0.01%), and ethylene glycol (<0.003%). Due to the hygroscopic nature of the reactants, all the reaction processes were carried out in a dry box or in a nitrogen atmosphere in order to maintain anhydrous conditions. All the glassware was dried overnight at 200 °C in order to remove surface water.

2.2 Synthesis of the phosphate precursor

The phosphate precursor was prepared by dissolving phosphorus pentoxide (P_2O_5) in anhydrous ethanol according to the stoichiometry of the following chemical equation:

$$P_2O_5 + 3EtOH \rightarrow OP(OEt)(OH)_2 + OP(OEt)_2(OH) \qquad (1)$$

The apparatus used for the synthesis is based on the previous work by Lee et al.[12] and by Ali et al.[13,14] The required amount of P_4O_{10} was added to a 100 ml three-neck round-bottomed flask fitted with a reflux condenser, gas inlet and a rubber septum, all in a controlled atmosphere glove box. This reaction setup was removed from the glovebox and connected to a nitrogen line to preserve the inert atmosphere. The appropriate volume of anhydrous ethanol was injected dropwise via a syringe through the rubber septum onto the P_2O_5 under vigorous magnetic stirring. Reaction (1) is highly exothermic and the use of an ice bath was necessary to minimize the loss of ethanol. The resultant solution was maintained under refluxing conditions at the boiling point of ethanol (78.5 °C) in a zero-grade nitrogen atmosphere for 24 h, and continuously magnetically stirred during the refluxing. The final product, a clear, pink, viscous liquid was then transferred to a dry box where all the subsequent sol–gel reactions were carried out.

2.3 Synthesis of the sol

The sols were synthesised using the alkoxide solution route. A solution of 4.60 g of calcium methoxide in 65.28 mL of ethylene glycol was magnetically stirred in a dry glove box for 24 h until a yellow, clear solution was obtained. Sodium methoxide was then added to this solution; a homogeneous solution was obtained after 10 min of stirring. This solution was then added dropwise to the ethylphosphate precursor under vigorous magnetic stirring. For the samples containing silica, tetraethoxysilane (TEOS) was added to this solution and after 30 min of stirring, water in a molar ratio TEOS : H_2O = 1 was added. The mixture was stirred at room temperature until complete dissolution had occurred (ca. 3 h). The final homogeneous, yellowish sol obtained was transferred into a plastic container, sealed and left in an oven at 90 °C. A flow diagram showing the preparation procedure is given in Fig. 1.

2.4 Drying and calcination of the gels

The gels were aged in the oven at 90 °C for 2 d and then dried at 150 °C for 48 h, ground and left at 180 °C for 48 h. The gels were then calcined in air at 400, 600 and 800 °C, achieved by heating to the target temperature at a rate of 0.5 °C min^{-1} and left at the final temperature for 2 h.

2.5 Characterisation

A liquid-state ^{31}P NMR spectrum on the precursor was collected using a NMR Jeol GSX 270 MHz; concentrated phosphoric acid (H_3PO_4 85%) was used as the reference. The liquid sample (ca. 1 mg) was put in a 5 mm diameter, high quality NMR tube containing a capillary with 99.9% deuterated dimethylsulfoxide (DMSO). The ratio of 1 : 10
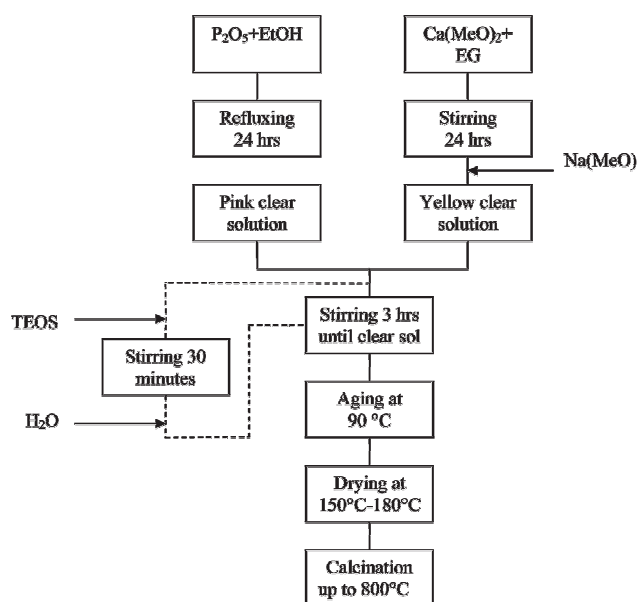
This journal is © The Royal Society of Chemistry 2005

J. Mater. Chem., 2005, 15, 2134–2140 | 2135

Fig. 1 Flow diagram of gel preparation

sample : solvent is typical for the analysis of 100% abundant nuclear species, *i.e.* ^{31}P, present in the sample. A Fourier transformation infra-red absorption spectrum of the precursor was recorded in the range 500–4000 cm^{-1} using a Bio-Rad FTS 175C FT-IR spectrometer. X-ray fluorescence chemical analysis (XRF) was carried out using a Bruker S4 Explorer with a Rh anode operating at 20 kV and 5 mA. X-ray diffraction (XRD) patterns were obtained on a Bruker D8 Advance with Cu Kα radiation (λ = 1.54 Å), operating at 40 kV and 40 mA. Scans were performed with a detector step size of 0.02° over an angular range 2θ = 5–50° and counting for 70 s per step.

3. Results and discussion

3.1 ^{31}P liquid NMR of the phosphate precursor

The ^{31}P NMR spectrum of ethanol reacted with P_2O_5 is reported in Fig. 2. The peaks around 0 ppm may be ascribed to phosphoric acid (1.5 ppm), mono- (0.2 ppm), di- (−1.2 ppm) and triethylphosphates (−2 ppm).[14] Mono- and diethyl-phosphates are present in approximately equal amount, while
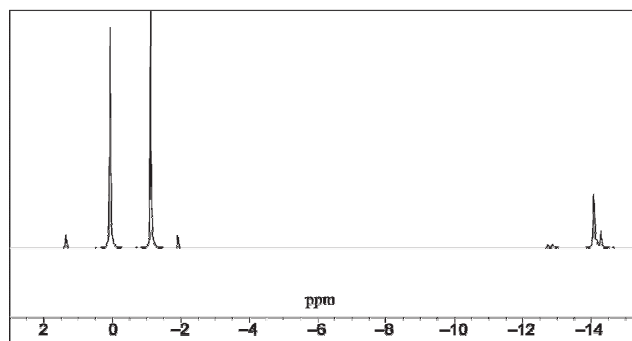
only a small amount of phosphoric acid and triethylphosphate can be observed. The peaks around −14 ppm may be assigned to the condensed phosphates. As reported by Ali *et al.*,[13] the presence of condensed phosphates is not a drawback during the sol–gel synthesis as they can hydrolyse and condense during the process. Furthermore, they may help to initiate the acidic hydrolysis of mono- and diethylphosphates. It is well known that the sol–gel hydrolysis can be catalysed by acidic or basic conditions. The condensed phosphates may help the initiation of the hydrolysis reaction because of their acidic character.

3.2 Infra-red analysis of phosphate precursor

In Fig. 3 the infra-red spectrum of the precursor after 24 h of refluxing is shown. O–P–O stretching signals are observed at 780 and 815 cm^{-1}. The symmetric and antisymmetric stretching of PO and PO_2 are observed between 950 and 1200 cm^{-1}. The broad band at *ca.* 3000 cm^{-1} is characteristic of OH groups. Sharp peaks corresponding to C–H groups can be observed in the same region.

3.3 Synthesis of the sol and gel formation

The common calcium and sodium alkoxide precursors are not soluble in the phosphate precursor solution. Thus, a stable mixed solution containing the calcium and the sodium precursor has to be prepared before addition to the phosphorus precursor: this condition is essential in order to obtain a clear and homogeneous sol after mixing with the phosphorus precursor, and one therefore needs to find a solvent that can dissolve both calcium and sodium precursors. Alcohols are often used as solvents in the sol–gel process as they can be easily removed from the gel by mild heating but they are not suitable in the present context. A series of solubility tests has been carried out at room temperature using a series of typical calcium sol–gel precursors in common alcohols. It transpired that the common calcium alkoxides have a very low solubility in alcohol. In previous work concerning the synthesis of
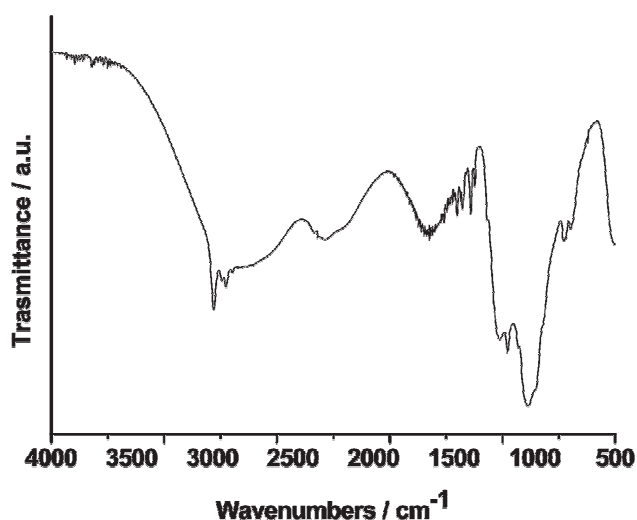

Fig. 2 ^{31}P liquid NMR spectrum of ethyl phosphate after 24 h refluxing P_2O_5 and ethanol.

Fig. 3 Infra-red spectrum of ethyl phosphate after 24 h refluxing P_2O_5 and ethanol.

calcium phosphates, Weng and Baptista used calcium granular[15] and calcium acetate[16] in ethylene glycol as a precursor solution. Refluxing was required to obtain a clear solution of calcium granular in ethylene glycol, and additional acetic acid was necessary to avoid the precipitation of calcium acetate solution with the phosphorus precursor.

In this work it has been found that ethylene glycol can dissolve both calcium and sodium methoxide at room temperature giving a clear sol after mixing with the phosphorus precursor. Table 1 shows a list of compositions of the synthesised sols. The samples containing more than about *ca.* 22 mol% of P do not gel, regardless of the amount of calcium and sodium alkoxides used. The condensation of the P–OH groups is promoted by the reactivity of the calcium and sodium alkoxides groups towards hydrolysis. As the ratio between phosphorous precursor and calcium and sodium methoxides in the sol increases, the number of OR groups (R = alkyl) may be not sufficient to promote the condensation process. The gelation time for the silicophosphates decreases with increasing silicon alkoxide content: the sols having *ca.* 2, 3 and 5 mol% of Si gel in 10, 8 and 6 d, respectively. The gelation times for the sols containing no silicon increase with increasing P content: varying from 8 d for the sol containing *ca.* 19 mol% P to 12 d for the ones having *ca.* 20 mol% and increases up to 18 d for the sols containing *ca.* 21 mol%, regardless of the amount of calcium and sodium alkoxides present. After aging in air at 90 °C for 2 d the gels appear clear and transparent. A picture of the gel of the composition: P_2O_5 45% CaO 30% Na_2O 25% (mol%) is shown as an example in Fig. 4.

3.4 XRF analysis of the calcined gels

One of the main problems in the sol–gel synthesis of phosphates glasses is the loss of phosphorus during the heating process. Szu *et al.*[11] found that the use of different phosphorus

Table 1 Compositions of synthesised sols and their gelation time

P (mol%)	Ca (mol%)	Na (mol%)	Si (mol%)	O (mol%)	Gelation time/d
18.6	7.0	14.0	—	60.4	8
18.8	8.2	11.8	—	61.2	8
19.0	9.5	9.5	—	62.0	8
19.6	4.3	15.2	—	60.9	12
20.0	6.6	11.1	—	62.3	12
20.1	7.9	9.0	—	63.0	12
20.4	9.1	6.9	—	63.6	12
20.7	10.3	4.6	—	64.4	12
20.0	6.7	6.7	2.2	64.4	10
20.2	7.7	4.5	2.5	65.1	10
20.2	9.1	2.3	2.3	66.1	10
19.6	4.3	8.7	3.3	64.1	8
20.0	6.6	4.4	3.3	65.7	8
20.5	9.1	—	3.4	67.0	8
19.1	2.0	7.9	5.0	66.0	6
19.5	4.3	4.3	5.4	66.5	6
20.0	6.6	—	5.5	67.9	6
21.2	6.4	8.6	—	63.8	18
21.5	7.5	6.5	—	64.5	18
21.7	8.7	4.4	—	65.2	—
22.2	11.1	—	—	66.7	—
22.5	6.2	6.2	—	65.1	—
22.7	7.2	4.1	—	66.0	—
22.9	8.3	2.1	—	66.7	—

Fig. 4 A picture of the as-synthesised gel with the composition: P_2O_5 45% CaO 30% Na_2O 25% (mol%).

precursors in the synthesis of P_2O_5–SiO_2 gels leads to different levels of loss of phosphorus upon heating. In Table 2, a list of the target compositions synthesised in the present work along with the results of X-ray fluorescence measurement is shown. The P, Ca, Na and Si in the sample names denote P_2O_5, CaO, Na_2O and SiO_2; the numbers following denote the mol% of each oxide. As the instrumental error is $\pm 0.1\%$, this suggests that there is a significant phosphorous loss. A possible reason for this is unreacted precursor being volatilize during heating.

3.5 XRD characterisation of the gels

All XRD diffraction patterns shown in this work refer to the gels listed in Table 2 after calcination at 400, 600 and 800 °C. Hereafter, the samples will be identified using their nominal composition. They contain 45 mol% P_2O_5 with 0, 10, 15 and 25 mol% SiO_2 and varying amounts of CaO and Na_2O. It is observed that all samples remained mainly amorphous up to 400 °C, and some of them retain their mainly amorphous nature up to 600 and 800 °C depending on the composition. The samples are considered amorphous if the powder pattern contains no discernable Bragg peaks. In Fig. 5 the XRD patterns of the samples without silica, calcined at 400 °C, are shown. The sample containing 30% of CaO is amorphous while the samples containing 35 and 40% show a partly crystallized calcium pyrophosphate, $Ca_2P_2O_7$, phase[17] in an amorphous matrix. The broad reflections indicate that the crystallites are quite small. As can be seen in Fig. 6, 7 and 8, the XRD patterns of the gels with 10, 15 and 25 mol% of silica are mainly amorphous after being heated at 400 °C regardless the amount of CaO and Na_2O.

Table 2 Intended compositions and compositions determined by XRF (in brackets) for gels after calcination at 400 °C

	P_2O_5 (mol%)	CaO (mol%)	Na_2O (mol%)	SiO_2 (mol%)
P45Ca30Na25	45 (39.8)	30 (33.0)	25 (27.2)	—
P45Ca35Na20	45 (40.9)	35 (44.0)	20 (15.1)	—
P45Ca40Na15	45 (40.4)	40 (45.4)	15 (14.2)	—
P45Ca30Na15Si10	45 (40.0)	30 (36.3)	15 (15.0)	10 (8.7)
P45Ca35Na10Si10	45 (40.6)	35 (39.9)	10 (10.1)	10 (9.4)
P45Ca40Na5Si10	45 (38.8)	40 (45.7)	5 (5.9)	10 (9.6)
P45Ca20Na20Si15	45 (40.5)	20 (27.8)	20 (18.0)	15 (13.7)
P45Ca30Na10Si15	45 (38.5)	30 (37.8)	10 (9.9)	15 (13.8)
P45Ca40Si15	45 (37.1)	40 (51.1)	—	15 (11.8)
P45Ca20Na10Si25	45 (38.5)	20 (28.8)	10 (9.2)	25 (23.5)
P45Ca30Si25	45 (42.6)	30 (36.4)	—	25 (21.0)

This journal is © The Royal Society of Chemistry 2005

J. Mater. Chem., 2005, **15**, 2134–2140 | 2137

1 $Ca_2P_2O_7$
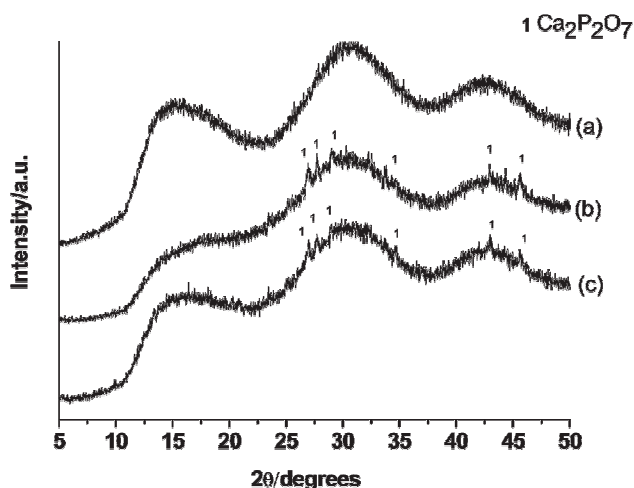
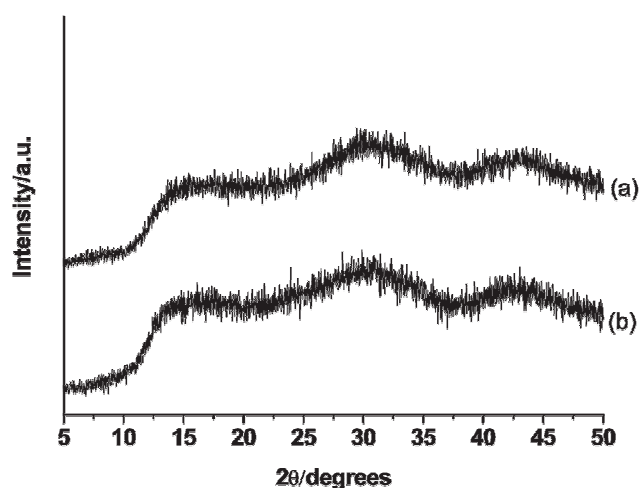Fig. 5 (a) P45Ca30Na25, (b) P45Ca35Na20, (c) P45Ca40Na15 (*i.e.*, samples containing no silica) at 400 °C.
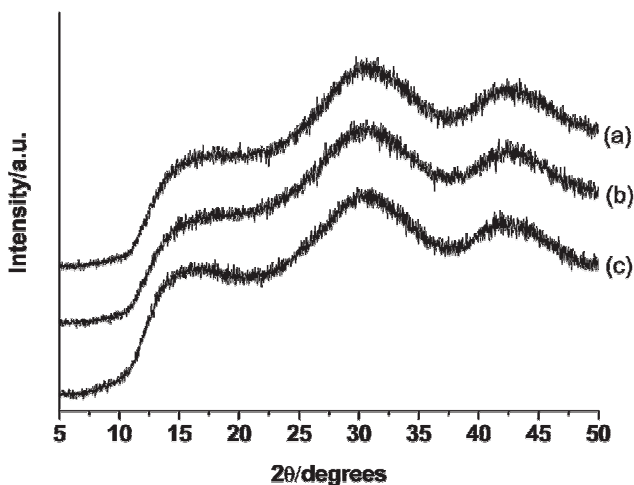

Fig. 6 (a) P45Ca30Na15Si10, (b) P45Ca35Na10Si10, (c) P45Ca40Na5Si10 (*i.e.*, samples containing 10 mol% of silica) at 400 °C.
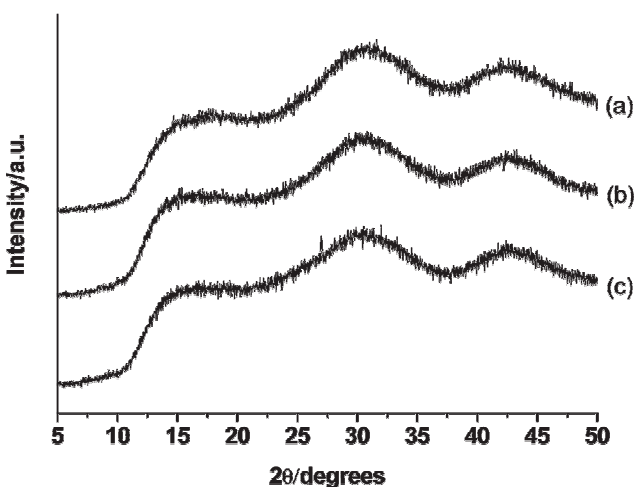

Fig. 7 (a) P45Ca20Na20Si15, (b) P45Ca30Na10Si15, (c) P45Ca40Si15 (*i.e.*, samples containing 15 mol% of silica) at 400 °C.

Fig. 8 (a) P45C20N10S25, (b) P45C30S25 (*i.e.*, samples containing 25 mol% of silica) at 400 °C.

In Fig. 9 and 10 the diffraction patterns of gels with 0 and 10 mol% of SiO_2 after calcination at 600 °C are shown. They are fully crystalline with a complex mixture of phases regardless of the amount of modifier oxides. As can be seen in Fig. 9, peaks corresponding to the $NaPO_3$ phase[18] can be observed in the samples without silica, and their intensity decreases as the amount of Na_2O decreases from 25 to 15 mol%. Peaks corresponding to a different sodium phosphate phase, $NaH_5(PO_3)_2$,[19] can also be observed. The others reflections can be ascribed to calcium pyrophosphate phases α-$Ca_2P_2O_7$,[20] β-$Ca_2P_2O_7$,[21] γ-$Ca_2P_2O_7$[22] and $CaH_2P_2O_7$.[23] They appear either as a single phase or as a mixture. Similar crystallisation behaviour is observed for the gels containing 10 mol% of SiO_2 (Fig. 10). The main difference is the precipitation of silicon-containing phases such as silicon phosphate $Si_3(PO_4)_4$[24] and calcium silicate $CaSiO_3$ (wollastonite).[25]

As the amount of silica increases from 10 to 15 mol%, the sharp peaks corresponding to the silicon-containing phase have almost disappeared apart from two weak reflections
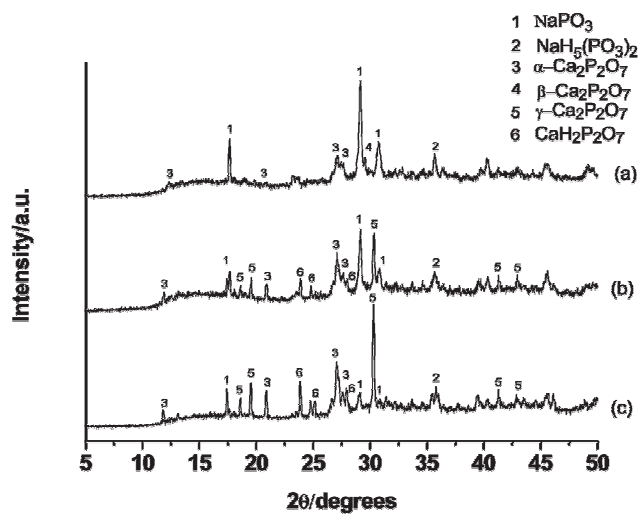

1 $NaPO_3$
2 $NaH_5(PO_3)_2$
3 α-$Ca_2P_2O_7$
4 β-$Ca_2P_2O_7$
5 γ-$Ca_2P_2O_7$
6 $CaH_2P_2O_7$

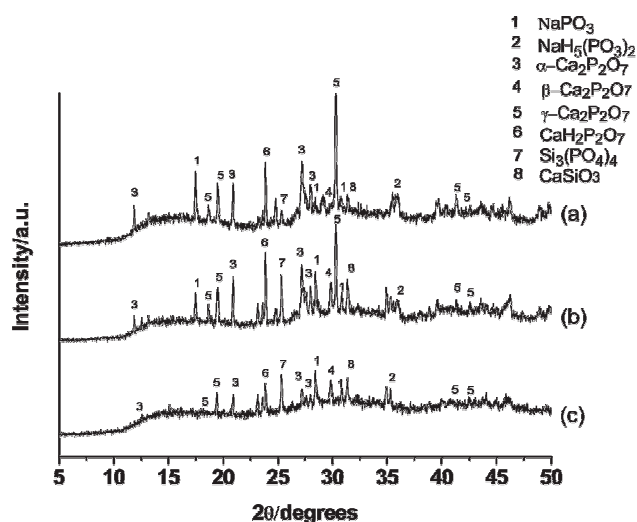Fig. 9 (a) P45Ca30Na25, (b) P45Ca35Na20, (c) P45Ca40Na15 at 600 °C.

Fig. 10 (a) P45Ca30Na15S10, (b) P45Ca35Na10S10, (c) P45Ca40Na5S10 at 600 °C.

observed in P45C30N10S15 sample (Fig. 11). The P45C40S15 sample, which does not contain Na_2O, appears predominantly amorphous. The amorphous nature is also the main feature observed in the samples containing 25 mol% of silica after heating at 600 C (Fig. 12). When heated at 800 C, a silicon pyrophosphate phase SiP_2O_7[26] appears in the sample P45C20N10S25 whereas the sample P45C30S25 remains amorphous (Fig. 13). These results suggest that the presence of silica in amount higher than 15 mol% moves the onset of the devitrification process to temperatures higher than 600 °C. Another interesting result is the absence of strong Bragg peaks in the samples containing no Na_2O. In absence of Na_2O, the calcium seems to remain incorporated in the amorphous phosphorus and silicon oxide network.

4. Conclusions

Glasses in the system P_2O_5–CaO–Na_2O–SiO_2 of low silica content (0–25 mol%) have been successfully synthesised using a
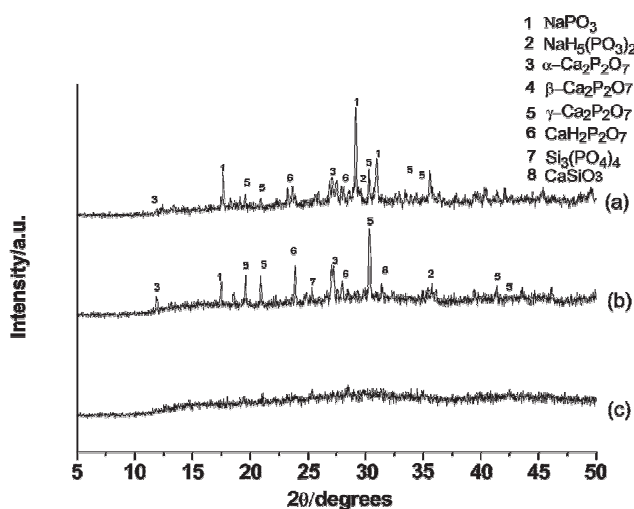

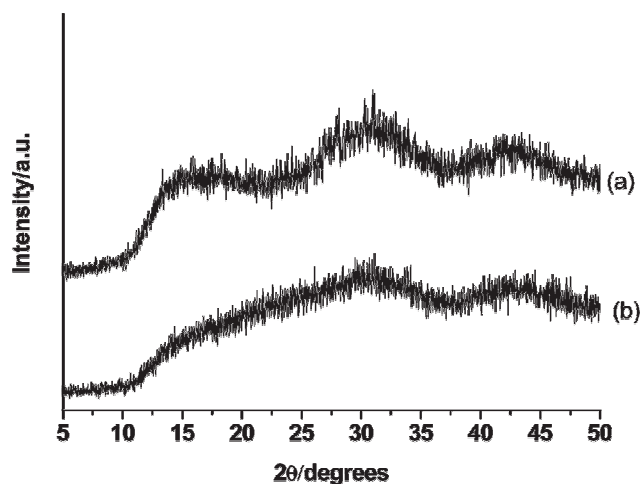Fig. 11 (a) P45Ca20Na20S15, (b) P45Ca30Na10S15, (c) P45Ca40S15 at 600 °C.

Fig. 12 (a) P45C20N10S25, (b) P45C30S25 at 600 °C.

novel sol–gel route. A mixture of approximately equal amount of mono- and diethylphosphates, prepared by dissolving phosphorus pentoxide in anhydrous ethanol, was used to generate a novel phosphate precursor. Ethylene glycol has been used as a solvent in order to obtain a homogeneous solution of calcium, sodium, silicon alkoxides and the phosphate precursor. The gelation time of the sol decreases with the increasing silicon alkoxide content for the silicophosphates, whereas it decreases with the decreasing phosphorus content for the pure phosphates. XRD measurements, performed on systems containing 45 mol% P_2O_5 with 0, 10, 15 and 25 mol% SiO_2 and varying amounts of CaO and Na_2O, show that all the samples are mainly amorphous after calcination at 400 °C for 2 h. Samples containing 25 mol% SiO_2 and 15 mol% SiO_2, in the absence of Na_2O, maintain their amorphous structure up to 600 °C. The sample containing 25% SiO_2, 20% CaO and 10% Na_2O crystallises after heating to 800 °C as SiP_2O_7 silicon pyrophosphate phase, whilst the samples with 25% SiO_2, 30% CaO and no Na_2O remain amorphous up to even 800 °C. All the other samples produced fully crystallize after calcinations
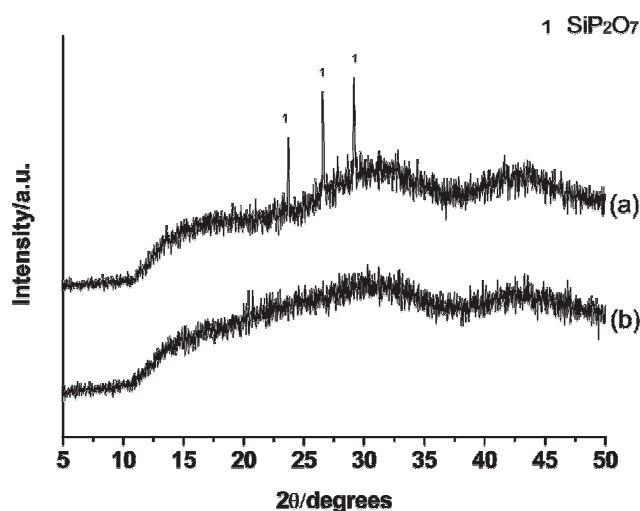

Fig. 13 (a) P45C20N10S25, (b) P45C30S25 at 800 °C.

This journal is © The Royal Society of Chemistry 2005

J. Mater. Chem., 2005, 15, 2134–2140 | 2139

at 600 °C showing evidence of the calcium pyrophosphate phases α, β, γ-$Ca_2P_2O_7$, and $CaH_2P_2O_7$ and the sodium phosphate phases $NaPO_3$ and $NaH_5(PO_3)_2$. In the phosphosilicate samples, additional phases of silicon phosphate $Si_3(PO_4)_4$ and calcium silicate $CaSiO_3$ (wollastonite) have been observed.

To our knowledge, this is the first time that phosphate-based glasses having these compositions have successfully been synthesised through the sol–gel method. In particular, there is no evidence of previous work showing amorphous phosphate sol–gels materials which do not contain either any silica or which contain less than 25 mol% of silica.

The novel sol–gel process described allows the production of phosphorus based materials that remain mainly amorphous even after significant heating. This route offers a new way of producing materials with the same composition as those that have already been proven biocompatible by *in vitro* studies using human cells of hard and soft tissue origin.[27] The biocompatibility of the sol–gel materials will be tested in the future.

Acknowledgements

Daniela Carta,[*a] **David M. Pickup,**[a] **Jonathan C. Knowles,**[b] **Mark E. Smith**[c] **and Robert J. Newport**[a]
[a]*School of Physical Sciences, University of Kent, Canterbury, UK CT2 7NR. E-mail: dc24@kent.ac.uk*
[b]*Eastman Dental Institute, University College London, 256 Gray's Inn Road, London, UK WC1X 8LD*
[c]*Department of Physics, University of Warwick, Coventry, UK CV4 7AL*

References

1 L. L. Hench, L. J. Splinter, W. C. Alen and T. K. Greenlee, *J. Biomed. Mater. Res.*, 1971, **2**, 117.
2 P. Saravanapavan and L. L. Hench, *J. Non-Cryst. Solids*, 2003, **318**, 1.
3 P. Saravanapavan and L. L. Hench, *J. Non-Cryst. Solids*, 2003, **318**, 14.
4 I. Ahmed, M. Lewis, I. Olsen and J. C. Knowles, *Biomaterials*, 2004, **25**, 491.
5 I. Ahmed, M. Lewis, I. Olsen and J. C. Knowles, *Biomaterials*, 2004, **25**, 501.
6 J. C. Knowles, K. Franks and I. Abrahams, *Biomaterials*, 2001, **22**, 3091.
7 T. Woignier, J. Phalippou and J. Zarzycky, *J. Non-Cryst. Solids*, 1984, **63**, 117.
8 M. Vallet-Regí, A. J. Salinas, J. Román and M. Gil, *J. Mater. Chem.*, 1999, **9**, 515.
9 N. J. Clayden, S. Esposito, P. Pernice and A. Aronne, *J. Mater. Chem.*, 2001, **11**, 936.
10 J. Livage, P. Barboux, M. T. Vandenborre, C. Schmutz and F. Taulelle, *J. Non-Cryst. Solids*, 1992, **147&148**, 18.
11 S. P. Szu, L. C. Klein and M. Geenblatt, *J. Non-Cryst. Solids*, 1992, **143**, 21.
12 B. I. Lee, W. D. Samuels, L. Q. Wang and G. J. Exarhos, *J. Mater. Res.*, 1996, **11**, 134.
13 A. F. Ali, P. Mustarelli and A. Magistris, *Mater. Res. Bull.*, 1998, **33**, 697.
14 A. F. Ali, P. Mustarelli, E. Quartarone and A. Magistris, *J. Mater. Res.*, 1999, **14**, 2.
15 W. Weng and J. L. Baptista, *J. Sol-Gel Sci. Technol.*, 1997, **8**, 645.
16 W. Weng and J. L. Baptista, *J. Eur. Ceram. Soc.*, 1997, **17**, 1151.
17 Powder Diffraction File, N° 01–0667.
18 Powder Diffraction File, N° 03–0688.
19 Powder Diffraction File, N° 37–0082.
20 Powder Diffraction File, N° 45–1061.
21 Powder Diffraction File, N° 09–0346.
22 Powder Diffraction File, N° 17–0499.
23 Powder Diffraction File, N° 37–0082.
24 Powder Diffraction File, N° 22–1380.
25 Powder Diffraction File, N° 76–0186.
26 Powder Diffraction File, N° 22–1321.
27 M. Bitar, V. Salih, V. Mudera, J. C. Knowles and M. P. Lewis, *Biomaterials*, 2004, **25**, 2283.